Quantum criticality and universal scaling of a quantum antiferromagnet

BELLA LAKE[1,2*†], D. ALAN TENNANT[2,3‡], CHRIS D. FROST[3] AND STEPHEN E. NAGLER[1]

[1]Condensed Matter Sciences Division, Oak Ridge National Laboratory, Oak Ridge, Tennessee 37831-6393, USA
[2]Department of Physics, University of Oxford, Clarendon Laboratory, Parks Road, Oxford OX1 3PU, UK
[3]ISIS Facility, Rutherford Appleton Laboratory, Chilton, Didcot, Oxfordshire OX11 0QX, UK
*Present address: Department of Physics & Astronomy, Ames Laboratory, IOWA State University, Ames, Iowa 50011, USA
‡Present address: Department of Magnetism (SF2), Hahn-Meitner Institute Berlin, Glienicker Str. 100, D-14109 Berlin, Germany
†e-mail: lake@ameslab.gov

Published online: 20 March 2005; doi:10.1327/nmat1327

Quantum effects dominate the behaviour of many diverse materials. Of particular current interest are those systems in the vicinity of a quantum critical point (QCP). Their physical properties are predicted to reflect those of the nearby QCP with universal features independent of the microscopic details. The prototypical QCP is the Luttinger liquid (LL), which is of relevance to many quasi-one-dimensional materials. The magnetic material $KCuF_3$ realizes an array of weakly coupled spin chains (or LLs) and thus lies close to but not exactly at the LL quantum critical point. By using inelastic neutron scattering we have collected a complete data set of the magnetic correlations of $KCuF_3$ as a function of momentum, energy and temperature. The LL description is found to be valid over an extensive range of these parameters, and departures from this behaviour at high and low energies and temperatures are identified and explained.

The concept of a quantum critical point[1,2]—a zero-temperature phase transition between quantum ground states—provides an attractive approach for describing regions dominated by quantum mechanics in condensed matter. In its vicinity, universal behaviours are predicted that are independent of the microscopic details of the system. An example of this is universal energy/temperature (E/T) scaling of the collective response of the system—a phenomenon that has received heightened attention due to its observation in both cuprate high-temperature superconductors[3–5] and unconventional metals[6–8]. By exploiting the powerful mathematics of scaling, the aim is to set up systematic expansions of the physical properties of these special points thus explaining the quantum-dominated behaviour found in a diverse range of systems. In quasi-one-dimensional quantum magnets, experimental and theoretical techniques[9] are now sufficiently advanced to study these ideas and methods in depth. Here we consider the generic problem of an array of one-dimensional systems weakly coupled together into three dimensions.

Quantum critical states in one-dimension (1D) are thought to apply to systems as diverse as carbon nanotubes, stripes in cuprate high-temperature superconductors, and spin chains[10,11]. The prototypical example is the spin-½ ($S = ½$) Heisenberg antiferromagnetic chain (HAFC), which maps onto the Luttinger liquid (LL) QCP. Here the magnetic ions possess spin angular momentum of ½, and interact with their nearest neighbours by antiferromagnetic Heisenberg exchange couplings in only one crystallographic direction. This system fails to develop long-range Néel ordering (where neighbouring spins point anti-parallel to each other) even at the lowest temperatures and has exceptional dynamical properties. The basic excitations are spinons[12], which are topological excitations that can be visualized as twists of π in the spin order. Spinons are fractional particles that possess spin values of $S = ½$, and because in quantum mechanics changes in angular momentum are restricted to integer units, only an even number of spinons can be created[13].

The multi-spinon excitation spectrum forms a continuum over an extended region of energy (E) and momentum or wavevector

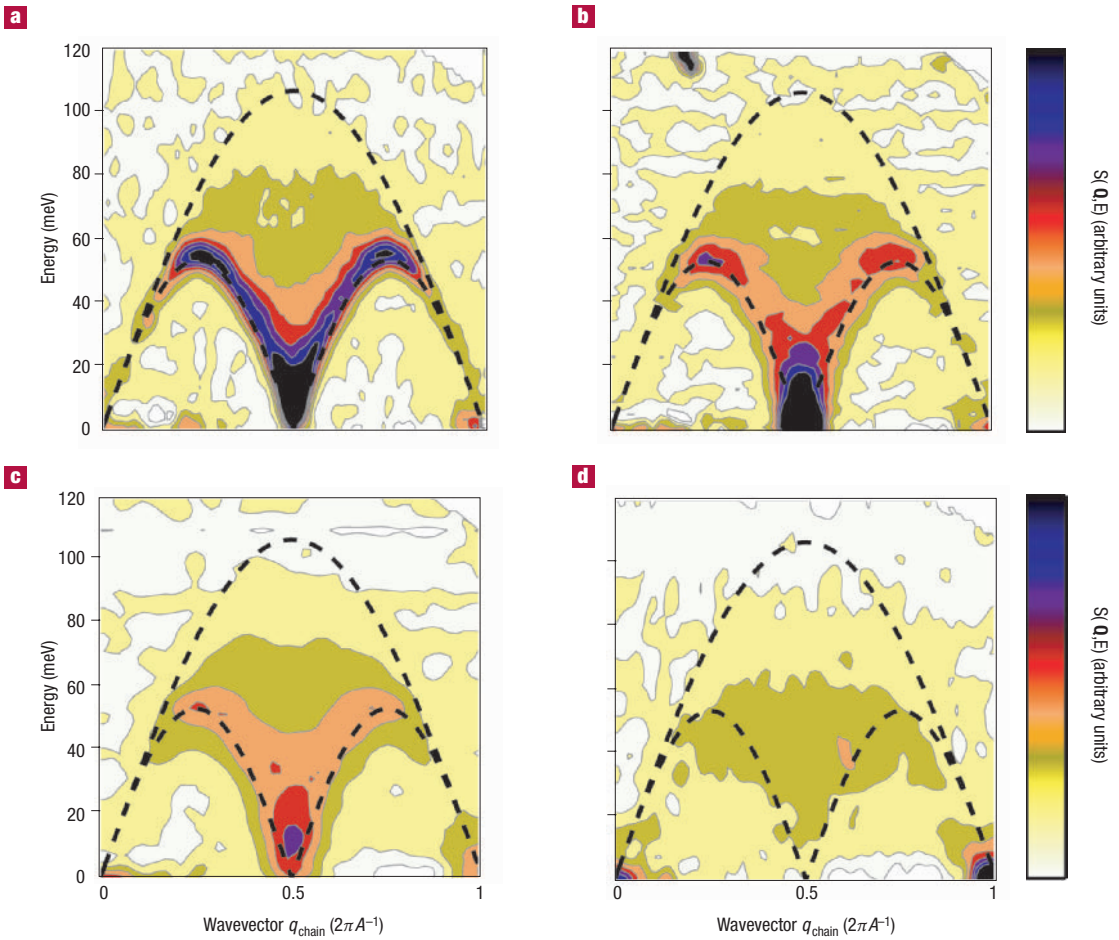

Figure 1 Inelastic neutron scattering data for $KCuF_3$. The data is plotted as a function of E and q parallel to the chains for the temperatures **a**, $T = 6$ K, **b**, $T = 50$ K, **c**, $T = 150$ K and **d**, $T = 300$ K. The colours indicate the size of the neutron scattering cross-section $S(q,E)$ and the superimposed black dashed lines indicate the region where the multi-spinon continuum is predicted at $T = 0$ K by the Muller Ansatz equation (1). The data was collected using the MAPS time-of-flight spectrometer at ISIS, Rutherford Appleton Laboratory, UK.

(q) space. The excitation spectrum is reflected in the dynamical structure factor probed by neutron scattering. At $T = 0$ K, this is given approximately by the Müller Ansatz equation[14]

$$S(q,E) = \frac{A_M \Theta(E - E_l(q)) \Theta(E_u(q) - E)}{\sqrt{E^2 - E_l^2(q)}} \quad (1)$$

where Θ is the Heaviside step function and A_M is a constant. The quantities E_l and E_u are the lower and upper energy boundaries of the continuum and are sinusoidal functions of wavevector given by

$$E_l(q) = \frac{\pi J}{2} \left| \sin(qc) \right| \text{ and } E_u(q) = \pi J \left| \sin\left(\frac{qc}{2}\right) \right| \quad (2)$$

where c is the lattice parameter in the chain direction and J is the antiferromagnetic exchange constant coupling nearest neighbours along the chain. The two-spinon contribution that dominates $S(q,E)$ has been calculated exactly[15], and found to extend between the same upper and lower boundaries, with an identical singularity at $E_l(q)$ and a smooth cutoff at $E_u(q)$. In order to develop the model for finite temperatures, field-theory techniques are used where the discrete lattice is approximated by a continuous medium. Schulz predicts that at the antiferromagnetic zone centre (AFZC) $q_{AFZC} = \pi/c$, the dynamical structure factor is given by

$$S(\pi,E) = \frac{e^{E/kT}}{e^{E/kT} - 1} \frac{A}{T} \mathrm{Im}\left[\rho\left(\frac{E}{4\pi T}\right)^2\right] \quad (3)$$

where $\rho(x) = \Gamma(1/4 - ix)/\Gamma(3/4 - ix)$ and A is a constant[16]. It is clear from this equation that the structure factor multiplied by temperature depends only on the dimensionless ratio of E to T rather than on these quantities separately, and therefore obeys universal scaling. The ideal $S = ½$ HAFC is rarely if ever found in the real world because inevitably any hamiltonian contains extra terms that have the potential to change the physical state; for example, even the smallest amount of interchain coupling alters the ground state and gives rise to Néel order (although with reduced ordered spin moment). The first problem we address in this paper is the experimental confirmation of the scaling specific to a 1D LL in a real material, which is close to but not at this QCP.

Dimensionality has important consequences for antiferromagnetism. For systems with nearest-neighbour exchange interactions this is evident from simple topological considerations, because the number of magnetic ions with which each spin interacts directly is an important factor in stabilizing long-range

order. The ideal 1D $S = ½$ antiferromagnet, with only two nearest-neighbours for each spin, fails to develop Néel order. Conversely, in the simple cubic 3D, $S = ½$ antiferromagnet where there are six nearest neighbours, mean-field effects lead to long-range order and the Néel state is often an adequate approximation to the true ground state. The excitations in the ordered state are spin-waves (Goldstone modes), which possess spin values of one and follow a well-defined trajectory in energy and wavevector[17,18] in complete contrast to the multi-spinon continuum. Quantum fluctuations are largely suppressed in this system and a semi-classical description in terms of the 3D nonlinear sigma model (NLσM)[19] is appropriate. The second problem that we address in this paper is the evolution of the magnetic correlation function with momentum, energy and temperature under the influence of interchain coupling.

To study these problems we investigate the magnetic excitation spectrum of the quasi-1D, $S = ½$, Heisenberg antiferromagnet $KCuF_3$. The magnetic Cu^{2+} ions carry $S = ½$ and are coupled into chains by a strong antiferromagnetic exchange interaction $J = 34$ meV, there is also a weak ferromagnetic exchange interaction $J_\perp = -1.6$ meV, which acts to couple these chains together[18,20]. The magnetic hamiltonian is

$$H = J\sum_{n,\mathbf{r}} \mathbf{S}_{n,\mathbf{r}} \cdot \mathbf{S}_{n+1,\mathbf{r}} + J_\perp \sum_{n,\mathbf{r},\delta} \mathbf{S}_{n,\mathbf{r}} \cdot \mathbf{S}_{n,\mathbf{r}+\delta} \qquad (4)$$

where n labels the sites along the chain, r represents a lattice vector lying in the plane perpendicular to the chains, and δ is summed over the four nearest neighbours in this plane. Magnetic ordering occurs below the Néel Temperature of $T_N = 39$ K with a saturated moment of 0.5 μ_B/Cu^{2+} at $T = 4$ K (ref. 20). The suppressed ordering temperature and moment reduction of 50% (from Néel ordering) show that despite the interchain coupling, $KCuF_3$ exhibits strong quantum fluctuations and is in the proximity of a QCP.

To measure the magnetic excitations in $KCuF_3$, we used the experimental technique of inelastic neutron scattering, for which the cross-section is directly proportional to the dynamical structure factor and can be used to probe it as a function of wavevector (1/distance) and energy (1/time) transfer. Figure 1 shows data collected over the full energy and wavevector range of the excitations at 6 K, 50 K, 150 K and 300 K (data was also collected at 75 K, 100 K, 200 K). The data are presented as a function of energy and wavevector parallel to the chains and are integrated over the two-dimensional Brillouin zone perpendicular to the chains. Figure 2b shows a detailed measurement at $T = 11$ K of the low-energy spectrum close to the antiferromagnetic zone centre. In all cases corrections have been made for background and the magnetic form factor of copper.

The data show that distinct regimes of behaviour occur in different regions of energy and temperature space. The extended scattering at high energies in Fig. 1a–c is similar to the excitation continuum of the 1D LL, indeed the scattering is bounded by the black dashed lines marking the theoretical upper and lower boundaries of the spinon continuum of a 1D $S = ½$ HAFC in its ground state given by the Müller Ansatz equation (1). Although this result might be expected at temperatures above the Néel temperature, it is clear that the continuum scattering is also present below T_N where long-range magnetic order develops. Figure 2 gives our complete data set for $T << T_N$. Although continuum scattering is present at most energies, detailed measurements made at low energies reveal highly dispersive V-shaped scattering (Fig. 2b) typical of the spin-waves of the 3D NLσM. Such coexistence of ID LL and 3D NLσM behaviour has been observed previously[21,22] in $KCuF_3$ and is a feature of the quasi-1D $S = ½$ HAFC; similar observations have been made in copper benzoate[23] and $BaCu_2Si_2O_7$ (ref. 24).

To test whether the 1D LL model is appropriate for $KCuF_3$ at high energies, the data was compared to the field theory result given by equation (3). The data was summed over the AFZC parallel to the chain direction ($0.48 < qc/2\pi < 0.52$) and integrated over the entire Brillouin zone perpendicular to the chain. This is plotted as a function of energy for the $T = 50$ K data in the inset of Fig. 3 and the solid line represents equation (3). Data lies on the theoretical curve for $26 < E < 80$ meV proving that the 1D LL description is valid over this energy range, however, the data fails to follow this theory at higher and lower energies. The data sets for other temperatures were treated in a similar manner and all of them except the 300 K data were found to follow the 1D LL expression over a large range of energies. In each case, the lower limit of this range was chosen as the energy below which two successive data points were more than 1.5 standard deviations above the fitted line. The main part of Fig. 3 shows the combined data for which the 1D theory gives an accurate description, multiplied by temperature and plotted as a function of the universal scaling parameter E/T, again the solid line is equation(3). What is remarkable is that although the data sets range in temperature from 6 K to 200 K they all lie on the same solid line with the same constant of proportionality A; that is, they depend only on the ratio of energy to temperature but not on these quantities independently. This result shows that the theoretical concept of the 1D LL strongly influences the physics of real magnetic systems that lie close to but not at this QCP due to a small amount of interchain

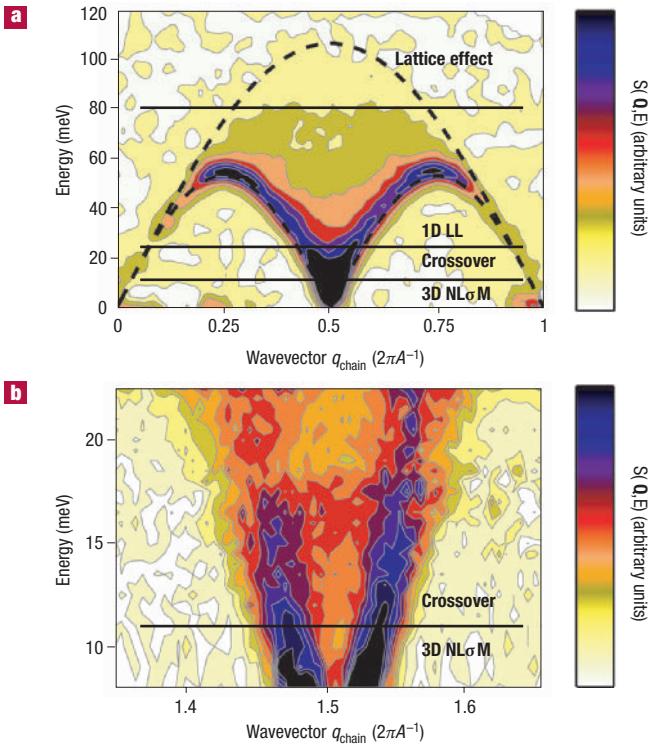

Figure 2 Inelastic neutron scattering data for $KCuF_3$ measured well below T_N and plotted as a function of energy and wavevector parallel to the chain direction. Again the colours indicate the size of the neutron scattering cross-section $S(q,E)$ and the superimposed black dashed lines indicate the region where the multi-spinon continuum is predicted at $T = 0$ K by the Muller Ansatz equation (1). The solid horizontal black lines are used to mark the energy ranges of the different regimes that exist at low temperatures, and these are labelled on the diagram. **a**, Data collected at $T = 6$ K using the MAPS time-of-flight spectrometer at ISIS, Rutherford Appleton Laboratory, UK. **b**, Data collected at $T < 11$ K using the HB1 triple axis spectrometer at HFIR, Oak Ridge National Laboratory, USA. The intensity scales on the two data sets are different.

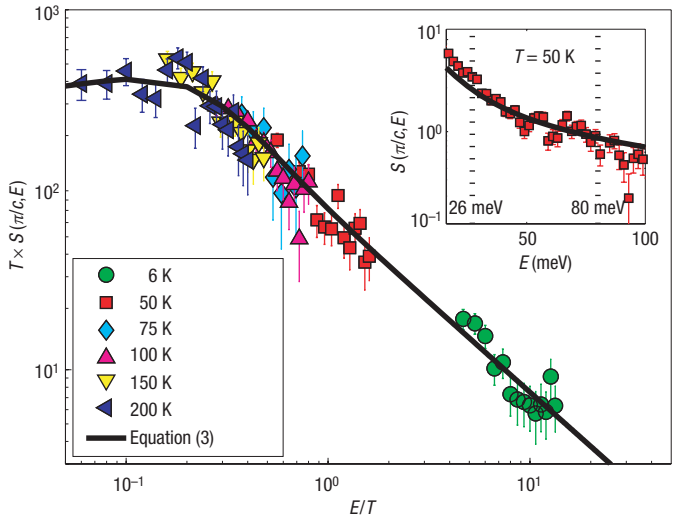

Figure 3 Universal energy/temperature scaling in $KCuF_3$. Inset: The corrected data at $T = 50$ K plotted as a function of energy. The data is integrated over the entire Brillouin zone perpendicular to the chain direction and summed over a narrow range at the AFZC parallel to the chain direction ($0.48 < qc/2\pi < 0.52$). The error bars represent two standard deviations. The solid line through the data is the field-theory expression for an ideal 1D $S = ½$ HAFC given by equation (3), which maps onto the 1D LL. The data follows this line for energies in the range $26 < E < 80$ meV (bounded by the vertical dashed lines) indicating that the 1D LL description is valid for $KCuF_3$ at these energies. Main figure: The data for all the other temperatures (except 300 K) were treated in a similar manner and were also found to follow equation (3) over a defined energy range. The combined data showing 1D LL behaviour is multiplied by temperature and plotted as a function of the universal parameter E/T in the main part of the figure. Again the solid line through the data is equation (3).

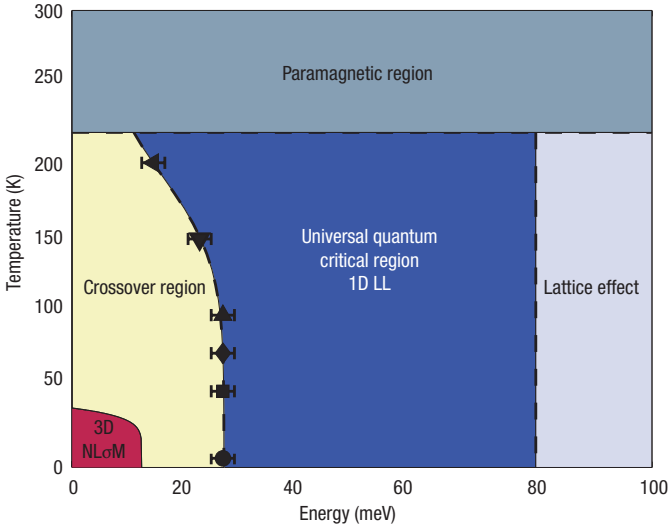

Figure 4 Magnetic crossover diagram showing the different physical regimes of $KCuF_3$ as a function of energy and temperature. The methods described in the caption of Fig. 3 and the text, have been used to identify the different magnetic regimes and the regions in energy and temperature that they occupy. In particular, the solid black symbols represents the lower energy limit of the 1D LL regime identified by the breakdown of scaling (see the inset of Fig. 3, which illustrates this for the $T = 50$ K dataset). The error bars are the instrumental resolution. The regimes are labelled on the diagram and the dashed lines mark the places where one phase crosses over into another.

coupling. It also clearly proves experimentally that the magnetic excitation spectrum of a material in this regime obeys universal E/T scaling over an extensive range of energies and temperatures.

The analysis described in the previous paragraph shows that by testing the magnetic excitation spectrum for scaling it is possible to identify not only whether a magnetic system behaves like a 1D LL, but also the energy and temperature ranges over which the QCP dominates. Thus this technique can be used to identify the different regimes of behaviour for the correlations of a quantum magnet, and construct a 'magnetic crossover diagram' showing where the different descriptions are dominant. Figure 4 shows this diagram for $KCuF_3$. Besides the 1D LL regime, it has also been possible to identify a 3D NLσM regime that occurs at low energies and temperatures and is bounded by an upper temperature of T_N above which long-range magnetic order is lost. The existence of this phase was established by measuring the sharpness of the excitations. δ-function modes, observed in neutron scattering as resolution-limited peaks, are a signature of spin-wave excitations and for the $T = 6$ K data they are found at energies of 11 meV and below. Above this, extra scattering is observed at the AFZC and the spin-wave model can no longer quantitatively account for the data. The scattering can be seen directly in Fig. 2b where, as energy transfer is increased at the AFZC, the intensity first decreases as the spin-wave branches disperse apart, however, above 11 meV the contours indicate an increase in the scattering intensity.

Although excitations with energies and temperatures that place them just outside the 3D NLσM regime cannot be explained by a spin-wave model, they also do not show the scaling behaviour of the 1D LL (equation (3)). We denote this intermediate state between the 3D NLσM and 1D LL regimes the crossover region (Fig. 4), because physically it corresponds to the onset of deconfinement where the $S = 1$ spin-waves begin to fractionalize into pairs of $S = ½$ spinons. This regime is characterized at low temperatures by the presence of a novel longitudinal mode—an excitation whose existence has only recently been established theoretically and experimentally[25–28]. The mode appears for $T < T_N$ lying at an energy of $E = 15$ meV (see Fig. 2b) and is broadened in energy with a full-width at half-maximum intensity of 5 meV (ref. 25), indicating a lifetime reduced by decay processes. The longitudinal mode is a crossover phenomenon existing in the presence of long-range magnetic order, but where the size of the ordered moment is significantly less than the full spin moment. Long-range order is required because longitudinal excitations are defined as oscillations in the length of this ordered moment, however if the full spin moment of each magnetic ion were to point along the ordering direction then these oscillations would clearly be restricted and their intensity negligible.

The ranges in energy and temperature occupied by the various regimes in $KCuF_3$ are very significant. Broadly speaking, the 1D LL description is valid at high energies and temperatures where the effects of interchain coupling become negligible, whereas the 3D NLσM description is valid at low energies and temperatures where the interchain interaction energy is similar to the thermal and excitation energies. The 3D NLσM regime exists for $T < T_N$ where long-range order occurs, and $E \leq 11$ meV where no longitudinal mode or spinon continuum scattering can be observed. Significantly, this energy is similar to $M = 11$ meV, the maximum (zone boundary) energy of the spin-waves perpendicular to the chain direction due to interchain coupling. The 1D LL regime occurs for $26 < E < 80$ meV (at $T = 6$ K). The lower limit of this regime is identified by the onset

of scaling and is similar to $2M = 22$ meV, which is the lowest energy that a spinon-pair must have if both spinons are to have energies greater than the perpendicular zone-boundary energy.

The upper edge of the 1D LL regime is also interesting and has its roots in the discrete nature of the crystal lattice. The 1D LL QCP maps directly onto the field theory expression (equation (3)). This equation, however, provides only an approximation to the behaviour of a $S = ½$HAFC where the discrete lattice has been replaced by a continuous medium so that the single-spinon excitation energies vary linearly with wavevector rather than sinusoidally as is the case for a lattice. This contrasts with the ground-state expression (equation (1)), which takes the lattice into account. The continuum assumption is adequate for wavevectors around the AFZC where the length scale of the excitations is much greater than the lattice spacing, but will clearly start to deviate away from the AFZC. Simulations suggest that the deviation is significant for wavevectors $|q-q_{\mathrm{AFZC}}| > 0.15 \times 2\pi/c$, for which the single-spinon energy is ~40 meV. The implication is that equation (3) can be expected to fail for energies greater that the corresponding spinon-pair energy of ~80 meV. It follows that 1D LL scaling is not obeyed above this energy. This is manifest in the measured data as a reduction in spectral weight at the highest energies compared with the predictions of equation (3). Figure 1a–c shows a drop in intensity (contour line) around $E = 75$–80 meV for all data sets except the $T = 300$ K data. This is a gradual crossover, and the upper limit of the 1D LL regime was set at ~80 meV, which is the average energy of all the data sets at which two consecutive points fall below the scaling expression by more than 1.5 standard deviations. Finally, as mentioned before, the scaling expression fails to account for any of the data collected at $T = 300$ K. The explanation for this is that thermal fluctuations dominate over quantum fluctuations at high temperatures and the magnetic response becomes paramagnetic. The Curie–Weiss temperature can be used as a rough guide to the onset of paramagnetism and for $KCuF_3$ it is calculated[29] to be $T_{\mathrm{Curie–Weiss}} = 216$ K using the experimental values for the exchange constants. At temperatures greater than this, thermal fluctuations are expected to destroy the 1D LL behaviour.

Our findings are consistent with QCP theory that has been modified to take account of interchain and other couplings[27]. The procedure is to map each magnetic chain onto a quantum 'string'[9] and use the powerful mathematics of conformal field theory to calculate quantities such as the collective response (equation (3)). This method can take into account all the relevant couplings that displace the $S = ½$ HAFC away from the quantum critical state. Essler, Tsvelik and Delfino (ETD)[27] have considered the coupling between chains in $KCuF_3$ and show that this particular operator acts to drive the system away from criticality, giving rise to magnetic order. They are able to calculate the response functions at $T = 0$ K using the method of form factors[30], and they find that in the ordered phase, the effect of ordered neighbouring chains is to confine spinons on long time and distance scales into 3D spin-waves below 11.5 meV, just as we find experimentally. Physically, this is because as spinons separate they leave overturned regions of spins that are mismatched with the order, this is expressible as a potential that confines spinons, which is proportional to their separation distance. ETD also predict a longitudinal mode, a novel type of bound mode of spinons, at 17 meV, which we indeed observe at the slightly lower energy of 15 meV in the crossover regime[25]. For energies above 22 meV, the response is expected to resemble the uncoupled 1D LL, because on these short timescales the spinons behave as if nearly free, which again corresponds to our findings. In fact, expansions around the 1D LL QCP account also to high accuracy for the size of the ordered spin moment and Néel temperature[28,31].

To conclude, by testing for scaling we have been able to construct the first magnetic crossover diagram of quasi-1D, $S = ½$ Heisenberg antiferromagnet, where the limits of the 1D LL regime are determined by the energies and temperatures where scaling breaks down, and the neighbouring phases have been identified and understood. Our measurements give firm experimental support to the QCP concept and show that it influences the behaviour of real materials that lie close to the QCP.

METHODS

The neutron scattering data shown in Fig. 1 and Fig. 2a was collected using the MAPS neutron scattering spectrometer at the ISIS neutron spallation source in the Rutherford Appleton Laboratory, UK. MAPS is a new state-of-the-art spectrometer with unprecendented detector coverage allowing large expanses of energy and wavevector space to be measured simultaneously to give the complete excitation spectrum. The crystal was aligned with its chains perpendicular to the incident neutron beam. A Fermi chopper was phased to select neutrons with an incident energy of 150 meV and was rotated at 500 Hz to provide an energy resolution of 5 meV. The sample was cooled in a closed cycle cryostat and was measured at a variety of temperatures from 6 K to 300 K, each temperature was collected for about a day (~3,000 μAmphr). The data shown in Fig. 2b was collected at $T = 11$ K using the HB1 triple-axis spectrometer at the High-Flux Isotope Reactor in Oak Ridge National Laboratory, USA[25]. The crystal was aligned so that chains lay in the horizontal scattering plane. The incident and final energies were selected using a monochromator and an analyser made of pyrolytic praphite (PG). The final energy was fixed at 13.5 meV and a PG filter was placed after the sample to remove higher order neutrons from the beam. A series of collimators with values 48′-40′-40′-120′ were used between the source and detector to provide an energy resolution of 1.3 meV and a wavevector resolution of 0.057 $Å^{-1}$ parallel to the chains at an energy transfer of 16 meV.

Received 21 April 2004; accepted 29 December 2005; published 20 March 2005.

References

1. Sachdev, S. Quantum criticality: competing ground states in low dimensions. *Science* **288,** 475–480 (2000).
2. Hertz, J. A. Quantum critical phenomena. *Phys. Rev. B* **14,** 1165–1184 (1976).
3. Keimer, B. *et. al.* Scaling behavior of the generalized susceptibility in $La_{2-x}Sr_xCuO_{4+y}$. *Phys. Rev. Lett.* **67,** 1930–1933 (1991).
4. Hayden, S. M. *et al.* Magnetic fluctuations in $La_{1.95}Ba_{0.05}CuO_4$. *Phys. Rev. Lett.* **66,** 821–824 (1991).
5. Aeppli, G., Mason, T. E., Hayden, S. M., Mook, H. A. & Kulda, J. Nearly singular magnetic fluctuations in the normal state of a high-T_C superconductor. *Science* **278,** 1432–1435 (1997).
6. Aronson, M. C. *et al.* Non-Fermi-liquid scaling of the magnetic response in $UCu_{5-x}Pd_x$ (x=1,1.5). *Phys. Rev. Lett.* **75,** 725–728 (1995).
7. Grigera, S. A. *et al.* Magnetic field-tuned quantum criticality in the metallic ruthenate $Sr_3Ru_2O_7$. *Science* **294,** 329–332 (2001).
8. Schroder, A. *et al.* Onset of antiferromagnetism in heavy-fermion metals. *Nature* **407,** 351–355 (2000).
9. Gogolin, A.,O., Nersesyan, A. A. & Tsvelik, A. M. *Bosonization and Strongly Correlated Systems* (Cambridge Univ. Press, Cambridge, 1998).
10. Luther, A. & Peschel, I. Single-particle states, Kohn anomaly, and pairing fluctuations in one dimension. *Phys. Rev. B* **9,** 2911–2919 (1974).
11. Luther, A. & Peschel, I. Calculation of critical exponents in two dimensions from quantum field theory in one dimension. *Phys. Rev. B* **12,** 3908–3917 (1975).
12. Faddeev, L. D. & Takhtajan, L. A. What is the spin of a spin-wave. *Phys. Lett. A* **85,** 375–377 (1981).
13. Haldane, F. D. M. Fractional statistics in arbitrary dimensions – a generalization of the Pauli principle. *Phys. Rev. Lett.* **67,** 937–940 (1991).
14. Muller, G., Thomas, H., Beck, H. & Bonner, J. C. Quantum spin dynamics of the antiferromagnetic linear chain in zero and nonzero magnetic field. *Phys. Rev. B* **24,** 1429–1467 (1981).
15. Karbach, M., Müller, G., Bougourzi, A. H., Fledderjohann, A. & Mütter, K.-H. Two-spinon dynamic structure factor of the one-dimensional S=1/2 Heisenberg antiferromagnet. *Phys. Rev. B* **55,** 12510–12517 (1997).
16. Schulz, H. J. Phase diagrams and correlation exponents for quantum spin chains of arbitrary spin number. *Phys. Rev. B* **34,** 6372–6385 (1986).
17. Anderson, P. W. An approximate quantum theory of the antiferromagnetic ground state. *Phys. Rev. B* **86,** 694–701 (1952).
18. Satija, S. K., Axe, J. D., Shirane, G., Yoshizawa, H. & Hirakawa, K. Neutron scattering study of spin waves in one-dimensional antiferromagnet $KCuF_3$. *Phys. Rev. B* **21,** 2001–2007 (1980).
19. Haldane, F. D. M. O(3) nonlinear sigma-model and the topological distinction between integer-spin and half-integer-spin antiferromagnets in 2 dimensions. *Phys. Rev. Lett.* **61,** 1029–1032 (1988).
20. Hutchings, M. T., Samuelsen, E. J., Shirane, G. & Hirakawa, K. Neutron-Diffraction Determination of the Antiferromagnetic Structure of $KCuF_3$. *Phys. Rev.* **188,** 919–923 (1969).
21. Tennant, D. A., Cowley, R. A., Nagler, S. E. & Tsvelik, A. M. Measurement of the spin-excitation continuum in one-dimensional $KCuF_3$ using neutron scattering. *Phys. Rev B* **52,** 13368–13380 (1995).
22. Tennant, D. A., Nagler, S. E., Welz, D., Shirane, G. & Yamada, K. Effects of coupling between chains on the magnetic excitation spectrum of $KCuF_3$. *Phys. Rev. B* **52,** 13381–13389 (1995).
23. Dender, D. C. *et al.* Magnetic properties of a quasi-one-dimensional S=1/2 antiferromagnet: Copper benzoate. *Phys. Rev. B* **53,** 2583–2589 (1996).
24. Zheludev, A. *et al.* Spin dynamics in the quasi-one-dimensional $S = 1/2$ antiferromagnet $BaCu_2Si_2O_7$. *Phys. Rev. B* **65,** 014402–014410 (2002).
25. Lake, B., Tennant, D. A. & Nagler, S. E. Novel longitudinal mode in the coupled quantum chain compound $KCuF_3$. *Phys. Rev. Lett.* **85,** 832–835 (2000).
26. Lake, B., Cowley, R. A. & Tennant, D. A. dimer model of the magnetic excitations in the ordered phase of the alternating chain compound $CuWO_4$. *J. Phys. Condens. Matter* **9,** 10951–10975 (1997).

27. Essler, F. H. L., Tsvelik, A. M. & Delfino, G. Quasi-one-dimensional spin-1/2 Heisenberg magnets in their ordered phase: correlation functions. *Phys. Rev. B* **56,** 11001–11013 (1997).
28. Schulz, H. J. Dynamics of coupled quantum spin chains. *Phys. Rev. Lett.* **77,** 2790–2793 (1996).
29. Kittel, C. *Introduction to Solid State Physics* 6th edn, 443–450 (Wiley, New York, 1986).
30. Smirnov, F. A. *Form Factors in Completely Integrable Models of Quantum Field Theory* (World Scientific, Singapore, 1992).
31. Bocquet, M. Finite temperature perturbation theory for quasi-one-dimensional spin-1/2 Heisenberg antiferromagnets. *Phys. Rev. B* **65,** 184415–184425 (2002).

Acknowledgements

We thank J. S. Caux, R. Coldea, F. H. L. Essler and A. M Tsvelik for helpful discussions and G. Shirane for the loan of the crystal. ORNL is operated by UT-Battelle LLC., under contract no. DE-AC05-00OR22725 with the US Department of Energy.
Correspondence and requests for materials should be addressed to B.L.

Competing financial interests

The authors declare that they have no competing financial interests.